Structure and magnetic order in $Fe_{2+x}V_{1-x}Al$

2001 J. Phys.: Condens. Matter 13 5487

(http://iopscience.iop.org/0953-8984/13/23/307)

INSTITUTE OF PHYSICS PUBLISHING JOURNAL OF PHYSICS: CONDENSED MATTER

J. Phys.: Condens. Matter **13** (2001) 5487–5501 www.iop.org/Journals/cm PII: S0953-8984(01)21514-8

Structure and magnetic order in $Fe_{2+x}V_{1-x}Al$

I Maksimov[1], D Baabe[1], H H Klauss[1], F J Litterst[1], R Feyerherm[2], D M Többens[2], A Matsushita[3] and S Süllow[1]

[1] Institut für Metallphysik und Nukleare Festkörperphysik, Technische Universität Braunschweig, 38106 Braunschweig, Germany
[2] Hahn-Meitner-Institut Berlin GmbH, 14109 Berlin, Germany
[3] National Research Institute for Metals, Tsukuba 305-0047, Japan

Received 30 January 2001, in final form 9 April 2001

Abstract

We present a detailed structural investigation via neutron diffraction of differently heat-treated samples of Fe_2VAl and $Fe_{2+x}V_{1-x}Al$. The magnetic behaviour of these materials is also studied by means of μSR and Mössbauer experiments. Our structural investigation indicates that quenched Fe_2VAl, exhibiting the previously reported 'Kondo-insulating-like' behaviour, is off-stoichiometric (6%) in its Al content. Slowly cooled Fe_2VAl is structurally better ordered and stoichiometric, and the microscopic magnetic probes establish long-range ferromagnetic order below $T_C = 13$ K, consistent with results from bulk experiments. The magnetic state can be modelled as being generated by diluted magnetic ions in a non-magnetic matrix. Quantitatively, the required number of magnetic ions is too large to be explained by a model of Fe/V site exchange. We discuss the implications of our findings for the ground-state properties of Fe_2VAl, in particular with respect to the role of crystallographic disorder.

1. Introduction

Recently, the magnetic phase diagram of the alloying series $(Fe_{1-x}V_x)_3Al$ has been the focus of various detailed studies [1, 2]. In particular, Heusler-type Fe_2VAl has been reported to exhibit a very unusual behaviour for an intermetallic compound, namely a semiconductor-like resistivity close to a magnetic instability [1]. This was interpreted in terms of Kondo insulating behaviour, analogous to the system FeSi [3, 4]. In contrast, optical conductivity studies provided evidence for a pseudogap in the density of states of Fe_2VAl of 0.1–0.2 eV [5], a view supported by various band structure calculations [6–8]. Notably, no temperature dependence of the gap features has been detected in these studies, apparently contradicting a Kondo insulator scenario for Fe_2VAl. However, the pseudogap scenario itself does not account for the unusual resistivity of Fe_2VAl, as in the absence of magnetic correlations it should predict no or a positive metallic magnetoresistance, in conflict with experimental observations [2, 9]. Therefore, in [5] it has been speculated that the (magneto) resistivity of Fe_2VAl reflects a

0953-8984/01/235487+15$30.00

mixture of electron excitation processes over the pseudogap and spin-dependent scattering from impurities.

Independently, on basis of specific heat and NMR experiments it has been demonstrated that, in Fe_2VAl, crystallographic disorder, assumed to be present in the form of atomic site exchange between Fe and V atoms, substantially affects the ground state properties of this compound [10, 11]. In particular, the anomalous low-temperature specific heat has been attributed to ferromagnetic clusters with a density of 0.003–0.004/unit cell, consistent with the results from NMR experiments. These works, as well, are in broad agreement with the results from band structure calculations, which predict that, via Fe/V site exchange or crystallographic superstructure formation, ferromagnetic clusters or long-range order might be generated in Fe_2VAl [6–8]. Recently, it has been claimed that such impurity-induced ferromagnetism was observed in the related Heusler compound Fe_2TiSn [12].

Matsushita and Yamada [13] found that the bulk properties of Fe_2VAl exhibit a very strong dependence on the applied heat treatment. They demonstrated that, by way of different cooling procedures after an annealing stage, the nature of the ground state of Fe_2VAl can be tuned; while quenched material exhibits the previously reported semiconducting-like, non-magnetic behaviour [1], a sample slowly cooled down to room temperature after a heat treatment shows almost metallic transport and a ferromagnetic transition at $T_C = 13$ K. Specific heat measurements assert the bulk nature of the magnetic transition in the slowly cooled samples.

In this context, the question arises whether any, or which, material—slowly cooled or quenched—Fe_2VAl represents the intrinsic behaviour of this compound. Based on the band structure, specific heat and NMR results, it would have to be argued that in slowly cooled material either a crystallographic superstructure has been formed [6] or that a larger level of Fe/V site exchanges is present [7, 8], both which might generate long-range magnetic order. Metallurgically, this is counter-intuitive, as the slow cooling procedure should allow the system a more complete relaxation from internal strain and non-equilibrium site occupations, compared to the freezing in of such forms of crystallographic disorder in the quenched material. Further, since ferromagnetism in slowly cooled Fe_2VAl is a bulk phenomenon, in the absence of a crystallographic superstructure it requires a drastic increase in the number of Fe/V site exchanged positions from the value in the quenched material, 0.003–0.004/unit cell, probably up to the level of the percolation limit, i.e. $\sim$10–20%, in slowly cooled samples. Such a strong dependence of the number of Fe/V site exchanges on the cooling procedure would require a critical re-examination of previous results on Fe_2VAl. Finally, if the resistivity, as suggested in [5], largely arises from spin-dependent scattering, then the very strong reduction of the resistivity in the slowly cooled sample seems to indicate a reduction of disorder scattering, in conflict with a view of impurity-induced ferromagnetism.

Given this contradictory experimental situation we decided to perform a thorough structural and magnetic investigation of slowly cooled Fe_2VAl, concentrating here on microscopic experimental techniques, complementary to the bulk experiments executed so far [13]. In particular, we performed a high-resolution neutron diffraction study and Mössbauer spectroscopy on slowly cooled and quenched Fe_2VAl. In addition, we performed similar investigations on other samples from the series $Fe_{2+x}V_{1-x}Al$, $x > 0$, in order to obtain reference data. Further, we studied slowly cooled Fe_2VAl by means of muon spin relaxation. We have chosen these techniques for the following reasons:

(a) If a crystallographic superstructure is formed in slowly cooled Fe_2VAl, it should be detectable in diffraction experiments. The contrast between Fe, V and Al in x-ray diffraction, because of their similar atomic weights, is weak, and might hinder the observation of a superstructure. Therefore, neutron diffraction experiments are more suitable, as Fe, Al and V have very different neutron scattering lengths yielding a high

contrast (Fe: 9.45×10^{-15} m; Al: 3.45×10^{-15} m; V: -0.38×10^{-15} m). Further, a superstructure might give rise to different local environments resolvable in Mössbauer spectra, i.e. in the form of a double-peak spectrum resulting from different isomer shifts at inequivalent lattice sites.

(b) ^{57}Fe-Mössbauer spectroscopy and muon spin relaxation are used to characterize the magnetic properties microscopically. In addition to long-range magnetic order these local probe techniques allow us to examine inhomogeneous magnetic states caused by crystallographic disorder. However, the expected size of the average magnetic moment in Fe_2VAl ($\sim0.1\mu_B$) is at the sensitivity limit of Mössbauer spectroscopy. Therefore, muon spin relaxation has been used as the most sensitive microscopic method to examine static magnetic order.

(c) If magnetic order stems from a large number ($\sim10\%$) of Fe/V site exchanged positions, with the high Fe/V contrast this should be resolved in a neutron diffraction experiment, and possibly in Mössbauer spectroscopy and muon spin relaxation studies.

(d) Repeating similar experiments for a number of samples $Fe_{2+x}V_{1-x}Al$, $x > 0$, enables us to compare the results for nominally ordered Fe_2VAl to those deliberately containing crystallographic disorder, thus allowing us to assess the relevance of disorder for the magnetic ground state of the systems.

We note that previously Mössbauer experiments have been performed on $Fe_{2+x}V_{1-x}Al$, $-0.1 \leqslant x \leqslant 1$ [14, 15]. In these works broad field distributions in the magnetically ordered state have been observed, which, however, have been interpreted in terms of magnetic fluctuations, in variance with the present view of long-range magnetic order. Further, the magnetic phase diagram determined in [15] differs greatly from that in [1, 16], thus adding to the inconsistencies, and Fe_2VAl was not specifically considered in these works.

2. Experiments and results

2.1. Metallurgy

Stoichiometric mixtures of the constituent elements Fe (4 N), V (3 N) and Al (5 N) have been arc-melted in a copper crucible under argon (5 N) atmosphere and simultaneous Ti-gettering [13]. The weight loss during this process was less than 0.5%. The specimens were cut from the polycrystalline ingot and sealed in evacuated quartz ampoules for the heat treatment. Initially, the two samples Fe_2VAl were homogenized at 1273 K for 24 h. The first sample (referred to as 'q-Fe_2VAl') was quenched in water after the heat treatment. The second one (referred to as 'sc-Fe_2VAl') was slowly cooled to 553 K at a rate of –6 K h^{-1}, and subsequently furnace cooled. Other samples $Fe_{2+x}V_{1-x}Al$ ($x = 0.5, 0.1, 0.02, 0.01$) were cooled down to 373 K at a rate of -60 K h^{-1} after homogenization at 1273 K for 15 h. Scanning electron microscopy (SEM) pictures have been taken of the samples, indicating that the materials consist of a homogeneous majority phase, with small inclusions of pure Al or Al oxides.

The samples have been characterized via resistivity and susceptibility, and for $Fe_{2+x}V_{1-x}Al$, $x = 0.5, 0.1, 0.02, 0.01$ and q-Fe_2VAl they exhibit the previously reported behaviour [1, 16], with a suppression of magnetic order and a tendency towards semiconductivity as $x = 0$ is approached. In contrast, sc-Fe_2VAl has a ferromagnetically ordered ground state and a more metallic resistivity, as reported in [13]. The transition temperatures, determined from the resistivity experiments, are: $x = 0.5$: $T_C > 300$ K; 0.1: $T_C = 28$ K, $x = 0.02, 0.01$ and q-Fe_2VAl: $T_C < 2$ K; sc-Fe_2VAl: $T_C = 13$ K.

2.2. Neutron scattering results

The structure of $Fe_{2+x}V_{1-x}Al$, $0 \leqslant x \leqslant 1$, derives from the cubic *DO3* lattice of Fe_3Al. In this lattice Fe occupies two inequivalent sites (figure 1(a)): Fe I on $(\frac{1}{2}\frac{1}{2}\frac{1}{2})$, and Fe II on $(\frac{1}{4}\frac{1}{4}\frac{1}{4})$ and $(\frac{3}{4}\frac{3}{4}\frac{3}{4})$, respectively. It is assumed that, for $x < 1$, the V ion almost entirely replaces Fe on the Fe I site [1]. For $x = 1$, that is for Fe_2VAl, this leads to a fully ordered Heusler lattice, with Fe, V and Al each occupying separate cubic sublattices. Band structure calculations [6–8] indicated that in Fe_2VAl each Fe ion occupying an Fe I site carries a magnetic moment. This requires a site exchange of V with an Fe II ion, which might cause, either via superstructure formation (i.e., V occupying exclusively one Fe II site) or a sufficiently large level of random Fe II/V site exchanges, a magnetically ordered state or anomalous behaviour from diluted magnetic clusters.

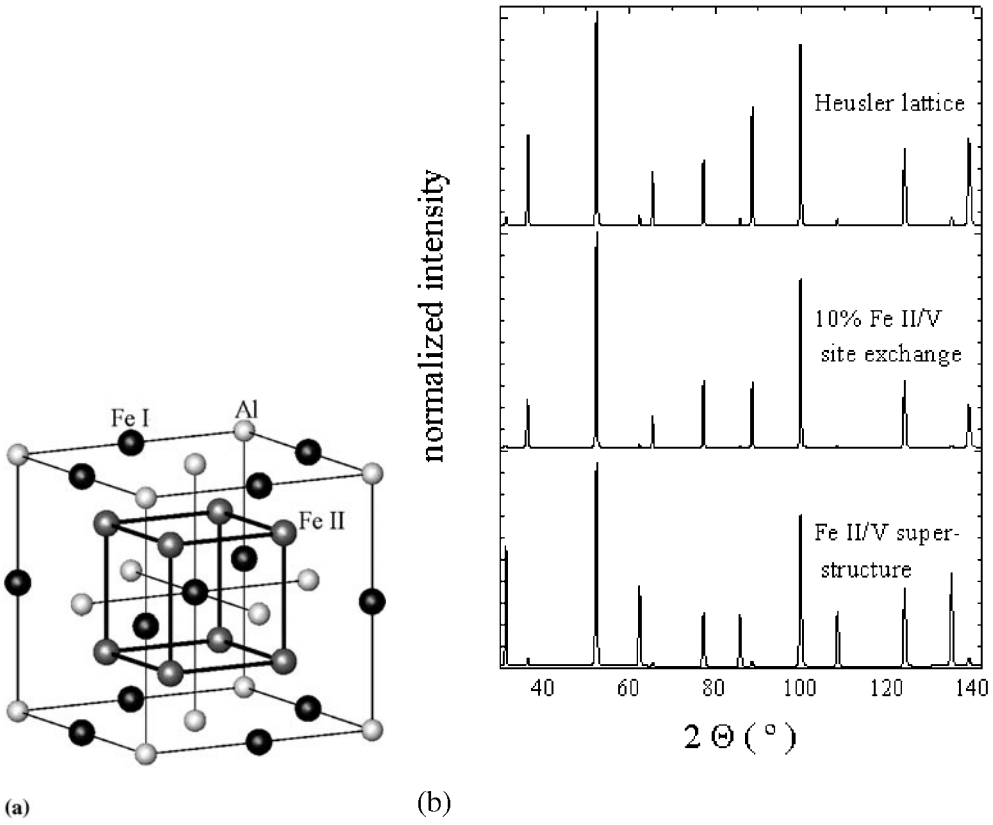

Figure 1. (a) The cubic *DO3* lattice of Fe_3Al, with the two inequivalent Fe sites at Fe I: $(\frac{1}{2}\frac{1}{2}\frac{1}{2})$ and Fe II: $(\frac{1}{4}\frac{1}{4}\frac{1}{4})$; $(\frac{3}{4}\frac{3}{4}\frac{3}{4})$. (b) The calculated normalized neutron diffraction intensities for the three different structural modifications Fe_2VAl: the fully ordered Heusler lattice (V on Fe I site), 10% Fe II/V site exchange and V entirely occupying one Fe II site, giving rise to a superstructure.

In figure 1(b) we plot the calculated neutron diffraction intensities for the above three structural modifications of Fe_2VAl: the fully ordered Heusler lattice, 10% random Fe II/V site exchange and a superstructure with V entirely occupying one Fe II site. Qualitative and quantitative differences between the calculated spectra are clearly visible, indicating that in a

high-resolution neutron diffraction experiment the level of Fe II/V site exchanged positions should be resolvable down to about 3% Fe on V sites.

Powder neutron diffraction data on $Fe_{2+x}V_{1-x}Al$, $0 \leqslant x \leqslant 0.5$, have been taken on the Fine Resolution Powder Diffractometer E9 of the Hahn–Meitner Institute (HMI) in Berlin [17]. The diffractograms have been recorded in the region $2\Theta = 5$–155°, with an incident neutron wavelength $\lambda = 1.7964(1)$ Å at temperatures $T = 50$ K. Full Rietveld structure refinements of the diffraction data were performed employing the program WinPLOTR/FULLPROF [18]. Typical results are presented in figure 2, where we plot the data for the sample with nominal composition $Fe_{2.1}V_{0.9}Al$. In the plot we include the refined fit, Bragg peak positions and the difference between fit and data. Spectra of similar high statistics have been taken for both samples (q- and sc-) of Fe_2VAl, and for $Fe_{2+x}V_{1-x}Al$, $x = 0.02, 0.5$.

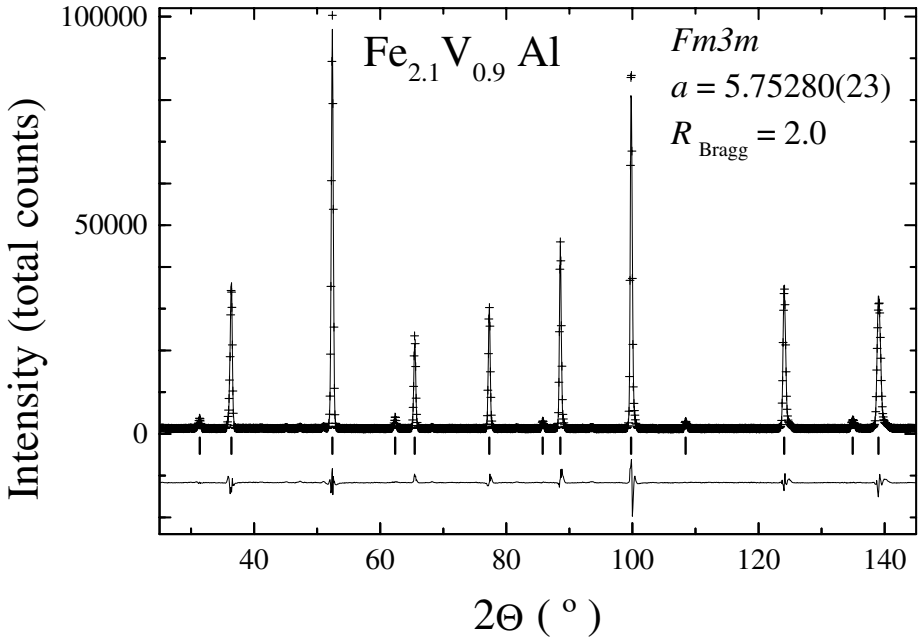

Figure 2. The neutron diffraction spectrum of $Fe_{2.1}V_{0.9}Al$, measured at 50 K (+). Included is a refined fit to the data, the difference between fit and data, and tics indicating Bragg peak positions.

All spectra correspond to the fully ordered cubic *Fm*3*m* Heusler structure with some site disorder; the formation of a crystallographic superstructure has not been detected for any sample. In addition, for all samples, between one and five Bragg peaks from an impurity phase, in addition to those reflections coming from the *Fm*3*m* lattice, have been observed. In view of the SEM results, the second phase is probably pure Al or Al oxide; the relative intensity of the corresponding Bragg peaks is low (between 0.3 to 1.3% for the largest peak), implying a small volume of this second phase (about 1%). We have tested if the refinements depend upon taking the secondary phase into account, but did not find a significant influence on the results. This reflects that the residual value of R_{Bragg} is almost completely determined by the mismatch between the fitted profile functions and the experimental data for the Bragg peaks of the cubic *Fm*3*m* phase.

More specifically, to refine our data, we used as input the cubic Heusler lattice, but modified it to incorporate different types of disorder: (a) assuming nominal composition;

(b) allowing for off-stoichiometry of Fe, V and Al; (c) considering possible site exchange between Fe, V and Al. Consistently, for all samples except for $Fe_{2.5}V_{0.5}Al$, the closest agreement between refinement and experimental data has been observed for models assuming Al off-stoichiometry. For $Fe_{2.5}V_{0.5}Al$ the models (b) and (c) did not yield a significantly improved solution compared to (a). Since $Fe_{2.5}V_{0.5}Al$ is ferromagnetically ordered ($\mu_{ord} = 0.85\mu_B$), magnetic scattering contributes to the spectrum. Yet, including a ferromagnetic scattering contribution in the refinement only marginally improved the fit. We stress that we could not find, for any of our samples, evidence for a significant level (>3%) of Fe II/V site exchange.

In table 1 we summarize the results of our refinements of the neutron diffraction data on $Fe_{2+x}V_{1-x}Al$, $0 \leqslant x \leqslant 0.5$. Overall, the refinements yield very good agreement with the experimental data, with R_{Bragg} values ~2% for $0 \leqslant x \leqslant 0.1$. The isotropic thermal displacement parameters B_{iso}, which for V we coupled to that of Al because of the small neutron scattering length of V, exhibit hardly any x dependence. In particular, no significant difference of the B_{iso} parameters for sc- and q-Fe_2VAl has been detected. However, lattice parameters and the measured compositions both show significant differences between the two samples Fe_2VAl.

Table 1. Summary of the refinement results of the neutron diffraction data on $Fe_{2+x}V_{1-x}Al$, $0 \leqslant x \leqslant 0.5$, with the cubic lattice parameter a, the isotropic thermal displacement parameters B_{iso} of Fe and V/Al, the measured composition and the value of R_{Bragg}.

Sample	Lattice parameter a (Å)	$B_{iso\text{-}Fe}$ (Å^2)	$B_{iso\text{-}V/Al}$ (Å^2)	Measured composition	R_{Bragg} (%)
$Fe_{2.5}V_{0.5}Al$	5.7604(3)	0.15(8)	0.9(2)	$Fe_{2.5}V_{0.5}Al$	4.3
$Fe_{2.1}V_{0.9}Al$	5.7528(2)	0.15(6)	0.3(2)	$Fe_{2.1}V_{0.9}Al_{1.01(5)}$	2.0
$Fe_{2.02}V_{0.98}Al$	5.7521(2)	0.13(6)	0.4(2)	$Fe_{2.02}V_{0.98}Al_{1.01(4)}$	2.1
sc-Fe_2VAl	5.7523(2)	0.25(6)	0.4(3)	$Fe_2VAl_{0.99(4)}$	1.9
q-Fe_2VAl	5.7514(2)	0.23(6)	0.3(3)	$Fe_2VAl_{0.94(4)}$	2.3

Previously, it has been reported that the lattice parameters of $Fe_{2+x}V_{1-x}Al$ are decreasing for decreasing x [1]. Specifically, while x was varying from 1 to 0.5 a linear variation of the lattice parameter with x was found, and subsequently a levelling off occurs as x approaches 0, until finally for $x < 0$ the lattice expands with x. This result is echoed in our experiments: upon reduction of x from 0.5 to 0.02 we observe a non-linear suppression of the lattice parameter a with x. This is illustrated in figure 3, where we plot the lattice parameters of $Fe_{2+x}V_{1-x}Al$ as a function of x. Remarkably, at $x = 0$, i.e., for Fe_2VAl, we find two significantly different values of a for slowly cooled and quenched material: for sc-Fe_2VAl it is about 0.02% larger than for q-Fe_2VAl. The relevance of this difference is indicated in figure 3: the construction with the dashed lines demonstrates that the value of the lattice parameter for sc-Fe_2VAl corresponds to that of $Fe_{2.05}V_{0.95}Al$. According to the phase diagram from [16] $Fe_{2.05}V_{0.95}Al$ is ferromagnetically ordered below $T_C = 15$ K. Therefore, we argue that the slow cooling procedure causes an expansion of the lattice in sc-Fe_2VAl, thus generating negative applied pressure and the onset of ferromagnetic order below $T_C = 13$ K.

The lattice parameter of q-Fe_2VAl falls out of the range of the other, more slowly cooled, samples. We believe that this reflects the significant Al off-stoichiometry of this sample. According to our data the actual composition is $Fe_2VAl_{0.94(4)}$, well out of the range of nominal stoichiometry. In contrast, for all other samples nominal and actual compositions are identical within the experimental uncertainty. More specifically, we directly compare the Bragg spectra measured for sc- and q-Fe_2VAl, after normalizing them for their overall intensities and correcting the latter for the angular shift from the difference in the lattice parameters. This

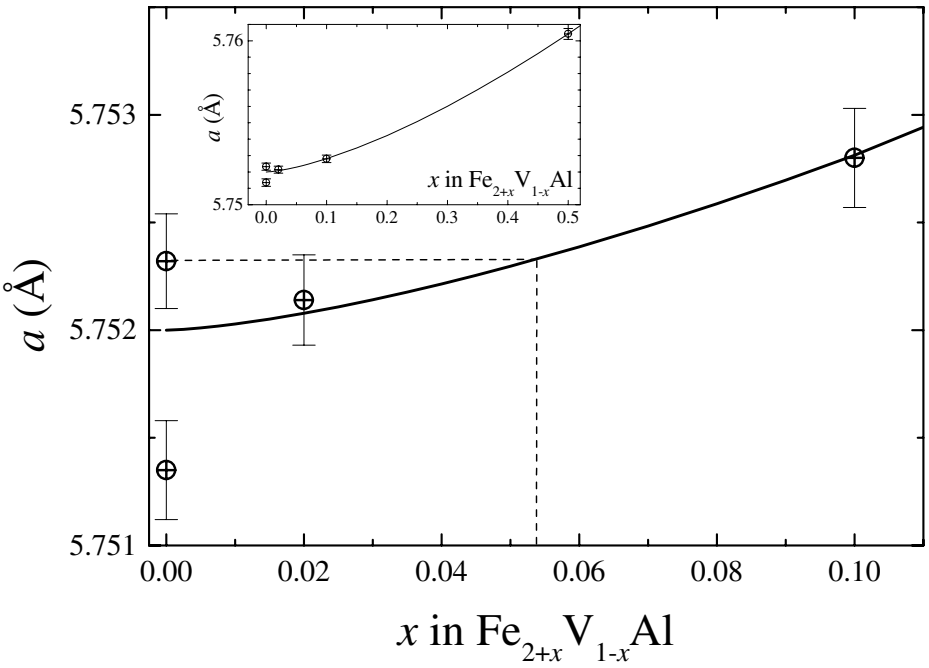

Figure 3. The lattice parameters of different samples $Fe_{2+x}V_{1-x}Al$, $0 \leqslant x \leqslant 0.1$, as a function of x. The inset depicts the data for $0 \leqslant x \leqslant 0.5$. Lines are guides to the eye.

procedure yields matching positions of the Bragg peaks of sc- and q-Fe_2VAl, as demonstrated in figure 4 for part of the spectra. We can directly determine the intensity difference between the two spectra $I_{\text{sc-Fe}_2\text{VAl}}$–$I_{\text{q-Fe}_2\text{VAl}}$, which is included in figure 4. Variations of the intensities for different Bragg peaks are resolvable for the two spectra. We quantify the intensity variations by calculating the relative difference of the areas, $1-\Sigma(I_{\text{q-Fe}_2\text{VAl}}(\Theta)/I_{\text{sc-Fe}_2\text{VAl}}(\Theta))\Delta\Theta$ under each Bragg peak. In figure 5 we present the result of this analysis, with the relative Bragg peak intensities for sc-Fe_2VAl in the lower panel, and the intensity variation in the upper one.

The $Fm3m$ Heusler lattice consists of four interpenetrating fcc sublattices with origins at A (000), B ($\frac{1}{4}\frac{1}{4}\frac{1}{4}$), C ($\frac{1}{2}\frac{1}{2}\frac{1}{2}$) and D ($\frac{3}{4}\frac{3}{4}\frac{3}{4}$). Bragg reflections are produced by either all even or all odd Miller indices with the three structure amplitudes:

$$F_1 \sim \left[(f_A - f_C)^2 + (f_B - f_D)^2\right]^{\frac{1}{2}} \qquad \text{for } h, k, l \text{ all odd}$$

$$F_2 \sim f_A - f_B + f_C - f_D \quad \text{for } \frac{1}{2}(h + k + l) = 2n + 1$$

$$F_3 \sim f_A + f_B + f_C + f_D \quad \text{for } \frac{1}{2}(h + k + l) = 2n$$

with n an integer, and $f_{A,B,C,D}$ as average scattering factors for the atoms A, C = Fe, B = V and D = Al, respectively. For identical stoichiometry of $I_{\text{sc-Fe}_2\text{Val}}$ and $I_{\text{q-Fe}_2\text{VAl}}$ no variation of the peak intensities $\frac{1}{2}(h + k + l) = 2n$ is expected. In contrast, experimentally we find for these peaks, on average, a larger intensity in sc-Fe_2VAl than in q-Fe_2VAl. This proves that a stoichiometry difference exists between the two samples. Further, for $\frac{1}{2}(h+k+l) = 2n + 1$ we find consistently that $I_{\text{sc-Fe}_2\text{VAl}} < I_{\text{q-Fe}_2\text{VAl}}$, which in view of the different $F3$ reflects that $f_{D:\text{q-Fe}_2\text{VAl}} < f_{D:\text{sc-Fe}_2\text{VAl}}$, i.e., a smaller Al concentration in the quenched sample compared to

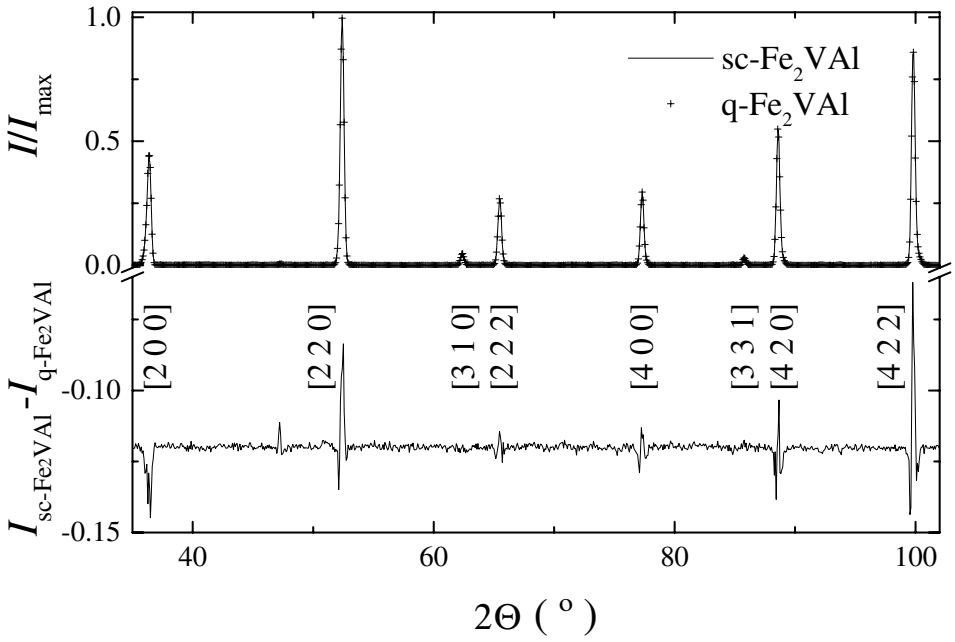

Figure 4. The normalized neutron spectra of sc- (solid line) and q-Fe_2VAl (+), and the difference $I_{\text{sc-Fe}_2\text{Val}} - I_{\text{q-Fe}_2\text{VAl}}$ between the two spectra.

sc-Fe_2VAl. Because of the comparatively small intensities of peaks $[h\ k\ l]$ = all odd, it yields a large error in the difference $I_{\text{sc-Fe}_2\text{VAl}} - I_{\text{q-Fe}_2\text{VAl}}$, prohibiting conclusions on the structural properties from the intensity variations of these peaks.

Refining the neutron spectra assuming stoichiometric composition Fe:V:Al = 2:1:1 yields for sc-Fe_2VAl a value $R_{\text{Bragg}} = 1.9\%$, which is significantly smaller than that of q-Fe_2VAl, $R_{\text{Bragg}} = 2.7\%$. Therefore, on basis of our neutron diffraction study of differently heat treated samples $Fe_{2+x}V_{1-x}Al$ we conclude that sc-Fe_2VAl, which is magnetically ordered below $T_C = 13$ K, structurally is much better ordered than q-Fe_2VAl. Primarily, the disorder in q-Fe_2VAl arises from Al vacancies, while Fe/V site exchange is not observable for any sample within the resolution of our experiment.

In addition to our structural investigation we attempted to study the magnetically ordered phases of sc-Fe_2VAl and $Fe_{2.1}V_{0.9}Al$ using the focusing diffractometer E6 at the HMI. We were unable to resolve intensity differences between measurements taken above and below T_C in our powder neutron diffraction experiments, indicating that for both sc-Fe_2VAl and $Fe_{2.1}V_{0.9}Al$ the ground states are ferromagnetically ordered with magnetic moments smaller than the resolution limit at E6 of about $0.5\mu_B$.

2.3. μSR-experiments

We performed time-differential muon spin relaxation experiments in zero external field (ZF-μSR) on the powdered specimen of slowly cooled sc-Fe_2VAl in the temperature range 3–225 K at the GPS spectrometer of the Paul Scherrer Institute, Switzerland. The sample was mounted with ultra-thin aluminium tape in a gas flow cryostat and electronic veto logic was used to register only the decay positron signals from muons stopped in the sample.

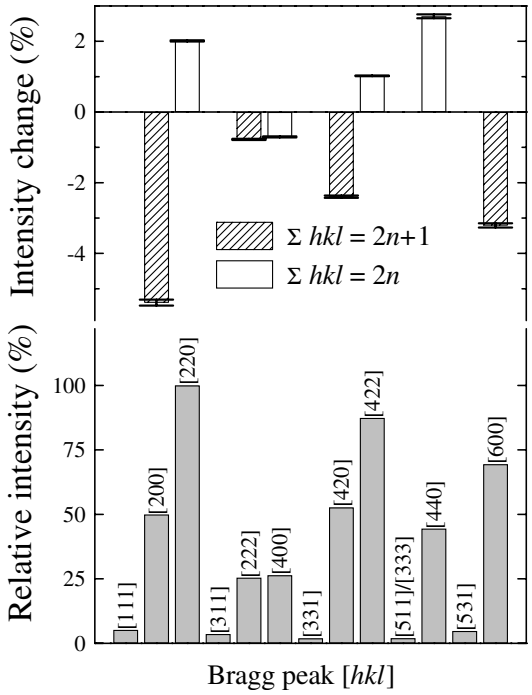

Figure 5. The relative Bragg peak intensities of sc-Fe_2VAl and the intensity variations, calculated from $1-\ \Sigma(I_{\text{q-Fe}_2\text{VAl}}(\Theta)/I_{\text{sc-Fe}_2\text{VAl}}(\Theta))\Delta\Theta$.

The muon spin polarization as a function of time is reconstructed by forming the asymmetry between the numbers of positrons emitted parallel and antiparallel to the original muon spin polarization direction. As described in [19] the experimentally determined asymmetry $A(t)$ is given as $A(t) = A_0G(t)$, where $A_0 \sim 0.21$ is the experimentally determined intrinsic asymmetry of the positron detectors and $G(t)$ the normalized polarization function of the muon ensemble implanted in the sample.

In zero external field possible sources for a relaxation of the muon spin ensemble are static local magnetic fields at the muon site, B_{loc}, due to finite electronic magnetic moments. The individual muon spin shows a Larmor precession around B_{loc} at a frequency $\omega_\mu = \gamma_\mu B_{\text{loc}}$, with $\gamma_\mu/2\pi = 13.55$ MHz kG^{-1}. For a magnetically ordered polycrystalline sample an isotropic spatial averaging over all angles between B_{loc} and the initial muon polarization $P_\mu(0)$ yields a polarization function $G(t) = \frac{1}{3} + \frac{2}{3}\cos(\omega_\mu t)\exp(-(\lambda_{\text{stat}}t)^\beta)$ [20]. The relaxation of the oscillating part describes an inhomogeneous distribution of B_{loc} for the total muon ensemble. If the average value of B_{loc} is zero and the form of the distribution is Gaussian, $G(t)$ is given by the Kubo–Toyabe function $G(t) = \frac{1}{3} + \frac{2}{3}(1 - \Delta^2t^2)\exp(-\frac{1}{2}\Delta^2t^2)$ [20]. In general, a static local field distribution in a polycrystalline sample will always lead to a longitudinal non-relaxing $\frac{1}{3}$ tail and a transverse relaxing $\frac{2}{3}$ signal fraction. If the field distribution becomes dynamic with a slow fluctuation rate $\nu \ll (\lambda_{\text{stat}}$ or $\Delta)$, the $\frac{1}{3}$ tail will exhibit a relaxation $\sim\exp(-\lambda_{\text{long}}t)$. For fast fluctuations ($\nu \gg (\lambda_{\text{stat}}$ or $\Delta)$) a single-component relaxation function $G(t) = \exp(-(\lambda_{\text{dyn}}\,t)^\beta)$ can be employed.

Typical ZF-μSR spectra of Fe_2VAl are depicted in figure 6. At temperatures below 13 K a two-component structure of a quasi-static spectrum exists: a fast relaxing transversal

part of nearly $\frac{2}{3}$ total signal amplitude and a slowly relaxing longitudinal part. No oscillating signal fraction is detected. Between 13 and 40 K the fast relaxing signal fraction gradually disappears and above 40 K only a single, slowly relaxing signal is observed.

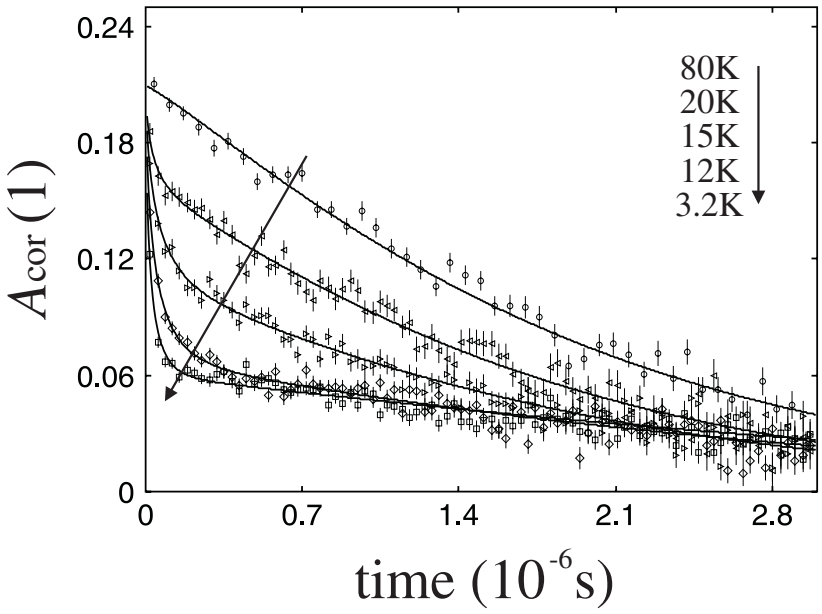

Figure 6. Zero field μSR spectra of sc-Fe_2VAl at different temperatures. The fit functions (solid lines) are described in the text.

The data sets can be described by a phenomenological polarization function of the form

$$A(t) = A_0\big(F_{\rm slow}\exp(-(\lambda_{\rm long}\,t)^{\alpha}\big) + (1 - F_{\rm slow})\exp\big(-(\lambda_{\rm trans}\,t)^{\beta}\big).$$

Common parameters at all temperatures are the spectrometer asymmetry $A_0 = 0.21$ and the generalized exponents $\alpha = 1.15(2)$ and $\beta = 0.64(3)$ describing the shape of the relaxation functions of the slow and fast components, respectively. The temperature dependence of the relative asymmetry $F_{\rm slow}$ of the slow component is plotted in figure 7, the resulting muon spin relaxation rates $\lambda_{\rm long}$ and $\lambda_{\rm trans}$ in figures 8 and 9.

The full signal amplitude in the temperature regime above 40 K reflects a paramagnetic relaxation of the muon spin. An additional 10% signal amplitude increase between 40 K and higher temperatures is attributed to a change of the experimental set-up (i.e., time resolution). The increase of the relaxation rate with decreasing temperature (figure 8) arises from the slowing down of the paramagnetic moments. Between 40 and 12 K the amplitude of this signal is gradually reduced and a strongly relaxing component appears, reflecting a sample volume fraction with quasi-static magnetic moments on a timescale of $\sim 10^{-7}$ s, e.g. inhomogeneous short-range magnetic order. The ordered volume fraction continuously increases from zero at $\sim$40 K to 100% at 12 K. The μSR data confirm a magnetic transition between 15 and 12 K, since the low-temperature value of $F_{\rm slow} = 0.29(2)$ clearly proves that below 13 K the sample is fully magnetically ordered. The 10% deviation of $F_{\rm slow}$ from the theoretical value $\frac{1}{3}$ is due to the constant sample amplitude fixed to the high temperature value above 40 K. The reduction of $\lambda_{\rm long}$ between 40 and 12 K reflects the change of the nature of the relaxation mechanism from dynamic, in the paramagnetic regime above 40 K, to a quasi-static one of the longitudinal muon

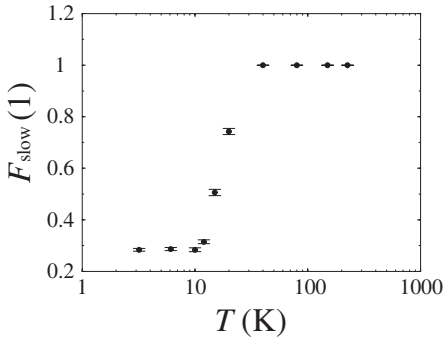

Figure 7. Temperature dependence of the slowly relaxing signal fraction F_{slow} in zero field μSR of sc-Fe_2VAl.

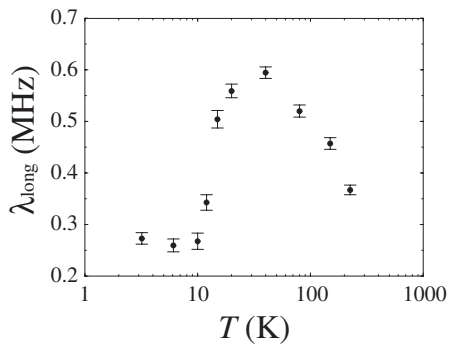

Figure 8. Temperature dependence of the longitudinal muon spin relaxation rate λ_{long} in zero field μSR of sc-Fe_2VAl.

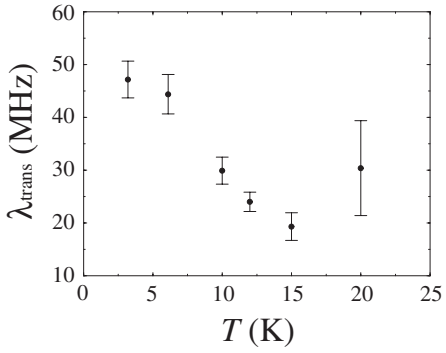

Figure 9. Temperature dependence of the transversal muon spin relaxation rate λ_{trans} in zero field μSR of sc-Fe_2VAl.

spin component in the magnetically ordered state. The saturation value of $\lambda_{long} \sim 0.27(2)\,\mu s^{-1}$ below 12 K corresponds in a strong collision model to an effective spin fluctuation rate of the same order. The very strong transversal relaxation rate λ_{trans} in the ordered state, and the absence of a coherent muon spin precession, indicate a rather inhomogeneous magnetic state with a broad local field distribution at the muon site. The increase of λ_{trans} with decreasing temperature is compatible with the increase of the magnetization at low temperatures. The value at 20 K corresponds to a strongly reduced signal asymmetry in the intermediate regime between the paramagnetic and ferromagnetic state and is not directly comparable with those at lower temperatures.

The fitted value of the shape exponent α is close to 1, the expected value for a quasi-static relaxation of the longitudinal signal fraction in the magnetically ordered state. In the paramagnetic regime this value is consistent with a homogeneous relaxation process with a Gaussian local field distribution and a well defined spin fluctuation rate. In the ordered state below 13 K the exponent β is significantly smaller than 1; this is usually observed in inhomogeneous magnets without spontaneous muon spin precession. In Fe_2VAl the main sources of the static field distribution are imperfections of the magnetic lattice caused by diluted lattice imperfections and impurities. In this case a Lorentzian field distribution (exponent $\beta = 1$) is expected for dominant dipolar or RKKY-type hyperfine

coupling between the muon and the local moments [21]. The observed behaviour is an indication of an inhomogeneous magnetic state causing a superposition of more than one lorentzian field distribution with different static widths. The μSR data cannot unambiguously clarify the cause for this inhomogeneity. Either size and orientation variations of small magnetic moments on each Fe site or diluted moments like those in a spin glass might be possible. Assuming the latter to be the case, we can compare the low-temperature saturation value of $\lambda_{\mathrm{trans}} \sim 47(3)\ \mu\mathrm{s}^{-1}$ to that of a canonical spin glass like (Au)Fe [22], where a linear scaling of λ_{trans} with the impurity spin concentration has been observed. From this comparison we obtain an impurity spin concentration of about 8(2)% in sc-Fe_2VAl. This value is consistent with the Mössbauer results presented below but incompatible with the upper bound for Fe II/V site exchange from neutron scattering.

2.4. Mössbauer spectroscopy

^{57}Fe Mössbauer spectroscopy experiments were executed on all samples $Fe_{2+x}V_{1-x}Al$, $0 \leqslant x \leqslant 0.5$, in a standard low-temperature Mössbauer set-up (source: ^{57}Co in Rh matrix) at temperatures ranging from 8 to 300 K. A full account of our experiments will be presented elsewhere [23]; here, we only address two aspects of our Mössbauer studies on $Fe_{2+x}V_{1-x}Al$.

In figure 10 we present the Mössbauer spectra of $Fe_{2.1}V_{0.9}Al$ measured at 50 and 10 K, together with the corresponding spectra of sc-Fe_2VAl at 50 and 8 K. The experiments at 50 K probe the paramagnetic state, while at 8/10 K the systems are ferromagnetically ordered. For both compounds similar Mössbauer spectra are observed: at 50 K we detect single lines with small isomer shifts of about 0.02–0.03 mm s^{-1}, relative to ^{57}Co(Rh), and linewidths (FWHM) $\Gamma = 0.22$ mm s^{-1} (solid lines in figure 10). Upon lowering the temperature below T_C a further broadening of the lines and a reduction of their depth occurs. The close quantitative and qualitative similarity between the temperature dependence of the Mössbauer spectra of $Fe_{2.1}V_{0.9}Al$ and sc-Fe_2VAl is emphasized by plotting the difference between the spectra at 50 and 8/10 K for both compounds (figure 10). It reinforces the notion of ferromagnetism in sc-Fe_2VAl as a result of the same mechanism as in $Fe_{2.1}V_{0.9}Al$ and is consistent with our view that it arises from negative chemical pressure.

For both $Fe_{2.1}V_{0.9}Al$ and sc-Fe_2VAl the observed behaviour is not the expected one for an archetypical bulk ferromagnet, since no well defined Zeeman splitting is visible. Previously, the Mössbauer spectra of $Fe_{2+x}V_{1-x}Al$ have been interpreted in terms of fluctuating spins [14, 15] and on basis of a 'shell model' of magnetic ions immersed in a non-magnetic matrix [9]. The first model is inconsistent with the observation of bulk ferromagnetic ordering for $Fe_{2.1}V_{0.9}Al$ and sc-Fe_2VAl.

The shell model has been successfully applied to disordered metallic ferromagnets like Fe–Al alloys [24]. It assumes that the hyperfine field at a given Fe ion results from a superposition of the contributions of magnetic ions sited in the nearest neighbour, next-nearest neighbour etc shell around the Fe ion. In $Fe_{2+x}V_{1-x}Al$ the magnetic ions are thought to be Fe II on V sites, which on the basis of band structure calculations are predicted to carry a large ($2\mu_B$) magnetic moment [6–8]. From our Mössbauer data we can estimate for sc-Fe_2VAl the required number of site exchanged Fe II/V pairs: to account for the broadening of the Mössbauer-line below T_C it would require at least 6% Fe II on V sites. This value, which is more than one order of magnitude larger than the estimated level of Fe/V site exchanges for q-Fe_2VAl of 0.3–0.4% [10, 11], is inconsistent with the result of our neutron diffraction experiments, setting an upper limit of 3% Fe II on V sites. Therefore, we conclude that neither model proposed so far properly accounts for the Mössbauer spectra of $Fe_{2+x}V_{1-x}Al$, $x \approx 0$.

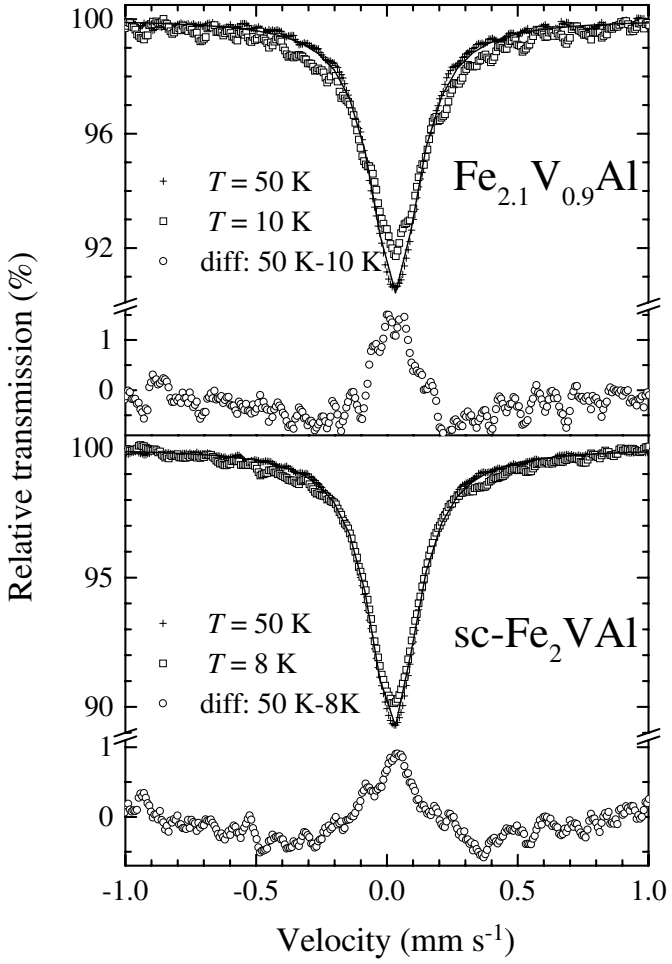

Figure 10. Mössbauer transmission spectra of $Fe_{2.1}V_{0.9}Al$ and sc-Fe_2VAl taken at 50 (+) and 10/8 K (□). Solid lines indicate single lorentzian fits to the 50 K data. Included in the plot are the differences between the spectra at 50 and 10/8 K (○), respectively.

3. Conclusions

We have presented powder neutron diffraction, μSR and Mössbauer experiments on $Fe_{2+x}V_{1-x}Al$ and, in particular, on differently heat treated samples of Fe_2VAl. Our structural investigation proves that slowly cooled Fe_2VAl, which we established on a microscopic scale to be ferromagnetically ordered below $T_C = 13$ K, is structurally better ordered than quenched material, for which we found evidence for substantial Al off-stoichiometry. For the quenched material the bulk properties [13] resemble the behaviour of 'Kondo-insulating-like' or 'pseudogap' Fe_2VAl [1, 2, 5, 9–11, 16]; this suggests that the materials investigated in those works are Al deficient.

As pointed out in [5], because of the electron count, Al deficiency might have a strong effect on the actual position of the Fermi level E_F in a pseudogap system. Specifically, it was argued that Al deficiency moves E_F out of the centre of the pseudogap into the slopes,

implying that Al deficient material should be more metallic than a non-deficient one. This hypothesis is in conflict with the observation that the resistivity of sc-Fe_2VAl is lower than that of q-Fe_2VAl, indicating less metallicity and E_F in the centre of the gap for the latter sample.

Another explanation for the smaller resistivity of sc-Fe_2VAl might be based upon the ability of Al vacancies to localize conduction electrons. Then, the resistivity of Fe_2VAl would depend strongly on disorder induced (i.e., from Al vacancies) localization of electrons in states close to the gap; with the larger degree of disorder in q-Fe_2VAl, its resistivity will be larger than that of sc-Fe_2VAl. Unfortunately, quantitative predictions are very difficult for this scenario, as it depends both on the actual position of E_F, because of the number of charge carriers from Al, and the strength and number of localizing potentials from Al vacancies. In addition, E_F might depend on the lattice parameter, i.e., the chemical pressure, which in turn is a function of the Al stoichiometry.

Altogether, we conclude that the physical properties, in particular the anomalous resistivity, of non-magnetic Fe_2VAl are dominated by crystallographic disorder. Kondo insulating behaviour seems not to play a role; specifically, Fe_2VAl can be easily turned into a ferromagnet, which is not expected for inherently non-magnetic Kondo insulators [25]. Further, we conclude that sc-Fe_2VAl is 'more representative' of the intrinsic behaviour of ambient pressure Fe_2VAl than quenched material, as it is closer to perfect stoichiometry. Hence, while the closeness to a pseudogap state predicted in band structure calculations [6–8] is found for both sc- and q-Fe_2VAl, the prediction of a non-magnetic ground state for stoichiometric, perfectly Heusler-ordered Fe_2VAl must still be considered a matter of debate. In particular, we note that, given our Mössbauer and μSR experiments, the simple view of 'Fe on the wrong (V) site' generating magnetism does not account for magnetic order in sc-Fe_2VAl, in so far as the measured number of 'wrong-sited' Fe is too low.

Since the properties of Fe_2VAl are so sensitively dependent on the actual stoichiometry, which is hard to control in the limits relevant to Fe_2VAl, we believe that pressure experiments on either sc-Fe_2VAl or q-Fe_2VAl represent a more fruitful route to study this material. Based on our experiments, for sc-Fe_2VAl we would expect a suppression of magnetic order upon application of pressure. For q-Fe_2VAl a pressure experiment might yield insight into the relevance of Al vacancies for electronic localization and the position of the Fermi level. Furthermore, pressure experiments might be very useful in combination with band structure calculations, as we would expect that the result of these calculations should sensitively depend on the value of the lattice constant.

Acknowledgment

Work at the TU Braunschweig was supported by the Deutsche Forschungsgemeinschaft DFG, under grant No SU 229/4-1.

References

[1] Nishino Y, Kato M, Asano S, Soda K, Hayasaki M and Mizutani U 1997 *Phys. Rev. Lett.* **79** 1909
[2] Endo K, Matsuda H, Ooiwa K, Iijima M, Goto T, Sato K and Umehara I 1998 *J. Magn. Magn. Mater.* **177–181** 1437
[3] Schlesinger Z, Fisk Z, Zhang H-T, Maple M B, DiTusa J F and Aeppli G 1993 *Phys. Rev. Lett.* **71** 1748
[4] Schlesinger Z, Fisk Z, Zhang H-T and Maple M B 1997 *Physica* B **237/238** 460
[5] Okamura H, Kawahara J, Namba T, Kimura S, Soda K, Mizutani U, Nishino Y, Kato M, Shimoyama I, Miura H, Fukui K, Nakagawa K, Nakagawa H and Kinoshita T 2000 *Phys. Rev. Lett.* **84** 3674
[6] Guo G Y, Botton G A and Nishino Y 1998 *J. Phys.: Condens. Matter* **10** L119
[7] Singh D J and Mazin I I 1998 *Phys. Rev.* B **57** 14352

[8] Weht R and Pickett W E 1998 *Phys. Rev.* B **58** 6855
[9] Matsuda H, Endo K, Ooiwa K, Iijima M, Takano Y, Mitamura H, Goto T, Tokiyama M and Arai J 2000 *J. Phys. Soc. Japan* **69** 1004
[10] Lue C-S and Ross J H Jr 1998 *Phys. Rev.* B **58** 9763
[11] Lue C-S, Ross J H Jr, Chang C F and Yang H D 1999 *Phys. Rev.* B **60** R13941
[12] Slebarski A, Maple M B, Freeman E J, Sirvent C, Tworuszka C, Orzechowska M, Wrona A, Jezierski A, Chiuzbaian S and Neumann M 2000 *Phys. Rev.* B **62** 3296
[13] Matsushita A and Yamada Y 1999 *J. Magn. Magn. Mater* **196/197** 669
[14] Popiel E S, Tuszynski M, Zarek W and Rendecki T 1989 *J. Less-Common Met.* **146** 127
[15] Popiel E S, Zarek W and Tuszynski M 1989 *Hyperfine Interact.* **51** 981
[16] Kato M, Nishino Y, Mizutani U and Asano S 2000 *J. Phys. Condens. Matter* **12** 1769
[17] Többens D M, Stüßer N, Knorr K, Mayer H M and Lampert G 2000 *Proc. 7th Eur. Powder Diffraction Conf. EPDIC 2000*
[18] Rodriguez-Carvajal J 1998 *WinPLOTR/FULLPROF* version 3.5d, Laboratoire Leon Brillouin–CEA-CNRS Oct98-LLB-JRC
[19] Nachumi B, Fudamoto Y, Keren A, Kojima K M, Larkin M, Luke G M, Merrin J, Tchernyshyov O, Uemura Y J, Ichikawa N, Goto M, Takagi H, Uchida S, Crawford M K, McCarron E M, MacLaughlin D E and Heffner R H 1998 *Phys. Rev.* B **58** 8760
[20] Dalmas de Réotier P and Yaounce A 1997 *J. Phys.: Condens. Matter* **9** 9113
[21] Walstedt R E and Walker L P 1974 *Phys. Rev.* B **9** 4857
[22] Uemura Y J and Yamazaki T 1983 *J. Magn. Magn. Mater* **31–34** 1359
[23] Baabe D *et al* in preparation
[24] Niculescu V, Raj K, Budnick J L, Burch T J, Hines W A and Menotti A H 1976 *Phys. Rev.* B **14** 4160
[25] Aeppli G and Fisk Z 1992 *Comment Condens. Matter Phys.* **16** 155